
PERGAMON

Journal of Quantitative Spectroscopy & Radiative Transfer 76 (2003) 69–83

Journal of Quantitative Spectroscopy & Radiative Transfer

www.elsevier.com/locate/jqsrt

Narrow-band and full-spectrum k-distributions for radiative heat transfer—correlated-k vs. scaling approximation

Michael F. Modest *

Department of Mechanical Engineering, The Pennsylvania State University, University Park, PA 16802, USA

Received 28 February 2002; accepted 14 March 2002

Abstract

The correlated-k and scaled-k distribution methods for radiative heat transfer in molecular gases are developed based on precise mathematical principles, for both narrow band and full spectrum models. Their differences and commonalities are high-lighted and discussed. Applications to narrow spectral bands of non-homogeneous gases show both methods to be about equally accurate. For full-spectrum calculations, on the other hand, the scaled-k distribution consistently outperforms the correlated-k model.

Keywords: Thermal radiation; Absorption coefficient; Molecular gases mixtures; Correlated-k; Scaling approximation

1. Introduction

Radiative transfer in absorbing–emitting gas mixtures can be most accurately predicted using the line-by-line approach, but LBL calculations require large computer resources and computational time. It has been known for some time that, for a narrow spectral range (i.e., a range over which the Planck function $I_{b\eta} \simeq const.$) in a homogeneous medium (i.e., absorption coefficient κ_η is not a function of spatial location), the absorption coefficient may be reordered into a monotonic k-distribution, which produces exact results at a tiny fraction of the computational cost [1,2]. As with other narrow band models, treatment of nonhomogeneous media was somewhat problematic. Two methods have been commonly used to address nonhomogeneity: the *scaling approximation* and the assumption of a *correlated k-distribution*. The former is somewhat more restrictive, by demanding that spectral and

* Tel.: +1-814-863-0976; fax: +1-814-863-8682.
E-mail address: mfm6@psu.edu (M.F. Modest).

0022-4073/02/$ - see front matter
PII: S0022-4073(02)00046-8

Nomenclature

a	weight function of k-distributions (dimensionless)
f_g	k-distribution (cm)
I, I_b	(blackbody) intensity (W/m^2 cm)
k_η	absorption coefficient at reference state (cm^{-1})
k	absorption coefficient variable at reference state (cm^{-1})
k^*	absorption coefficient variable at other state (cm^{-1})
L	length (cm)
L_m	mean beam length (cm)
p	pressure (bar)
$\hat{s}$	unit direction vector (dimensionless)
T	temperature (K)
u	scaling function for absorption coefficient (dimensionless)
V	volume (cm^3)
x	mole fraction (dimensionless)

Greek

κ_η, κ_P	spectral or Planck-mean absorption coefficient (cm^{-1})
η	wavenumber (cm^{-1})
σ_s	scattering coefficient (cm^{-1})
Φ	scattering phase function (dimensionless)
$\underline{\phi}$	composition variable vector $\underline{\phi} = (T, p, \underline{x})$
Ω	solid angle (sr)

Subscripts

0	reference state
k	at a given value for the absorption coefficient variable
g	at a given value for cumulative k-distribution
η	at a given wavenumber

spatial dependence of the absorption coefficient be separable, i.e.,

$$\kappa_\eta(\eta, \underline{\phi}) = k_\eta(\eta) u(\underline{\phi}), \tag{1}$$

where $\underline{\phi}$ is a vector containing the composition variables that affect the absorption coefficient (temperature T, pressure p, and mole fractions $\underline{x}$). An advantage of the scaling approximation is that mathematical expressions for nonhomogeneous media k-distributions can be readily obtained. In the correlated k-distribution method it is assumed that the maximum absorption coefficients across the spectrum under investigation always occur at the same wavenumber, regardless of composition

variables $\underline{\phi}$, and similarly for all intermediate values. This implies that the nondimensional, reordered wavenumber g (or cumulative k-distribution) corresponds to identical sets of actual wavenumber locations η, regardless of $\underline{\phi}$. While less restrictive than the scaling approximation (a scaled absorption coefficient always results in correlated k-distributions, but not vice versa), it has not yet been formulated in precise mathematical terms. The method has been shown to be of great accuracy in meteorological applications, which are governed by strong total pressure variations (from atmospheric to very low pressures at high altitude), and only small temperature changes (perhaps between 200 and 300 K) [1,3,4]. If temperatures are relatively uniform, this implies that the same spectral lines contribute to the radiative transfer everywhere, but that these lines have strongly varying widths at different pressures (altitude); nonetheless, maxima of the absorption coefficients (at the line centers) are the same everywhere, and it is not surprising that the assumption of a correlated absorption coefficient gives extremely accurate result, indeed more accurate than the heretofore popular Curtis–Godson narrow band approximation (based on a scaled absorption coefficient).

The situation is reversed in high-temperature combustion applications, which generally operate at relatively constant total pressure, but which are accompanied by extreme changes in temperature and concentration levels. Spectral lines from higher vibrational levels are negligible at room temperature but, with rising temperature, higher vibrational levels become more and more populated giving rise to so-called "hot lines". For example, the HITRAN96 database [5] contains 75,000 lines for CO_2 (valid up to 600 K), while the HITEMP database [6] (valid up to 1000 K) contains almost an additional 1,000,000 lines! Therefore, at significantly different temperatures, totally different spectral lines dominate the radiative transfer, and the assumption of a correlated absorption coefficient breaks down. This was first recognized by Rivière et al. [7–9]. Similarly, in a mixture of gases the correlation breaks down in the presence of strong, independent changes in concentrations, as recognized by Modest and Zhang [10], i.e., at one spatial location the absorption coefficient may be dominated by one specie, and by another (with totally different lines) at a different location. For such cases the scaling approximation can produce superior results, since the scaling function can be optimized for the problem at hand.

More recently, the reordering concept has also been applied to the full spectrum. Denison and Webb [11,12] developed the spectral-line-based weighted-sum-of-gray-gases (SLW) model, in which line-by-line databases are used to calculate weight factors for the popular WSGG model [13,14]; for nonhomogeneous gases they used the correlated-k approach. A similar method, called the absorption distribution function (ADF) approach, was developed by Rivière et al. [15,16]. Very recently, Modest and Zhang [10] demonstrated how k-distributions can be obtained for the entire spectrum, calling it the FSCK method. Their approach differs from the SLW and ADF approaches in two respects: (1) they obtained a continuous k-distribution, rather than the stepwise WSGG method [showing that the SLW/ADF/WSGG methods are crude step implementations of the full-spectrum k-distribution (FSCK) method]; and (2) they used the scaling approximation, to make a clear mathematical development of the method possible for inhomogeneous media. In addition, they introduced a somewhat more elaborate scheme for establishing a reference state, which further improves accuracy.

It is the purpose of the present paper (a) to show that a precise mathematical formulation is possible also for correlated-k distributions (for narrow bands as well as for the entire spectrum), and (b) to compare the accuracy of the two approaches in the context of narrow band transmissivities as well as the full-spectrum k-distribution applied to a water vapor–carbon dioxide mixture.

2. Theoretical analysis

2.1. Narrow band analysis

Consider the radiative transfer equation (RTE) for an absorbing, emitting and scattering medium [17]:

$$\frac{\mathrm{d}I_\eta}{\mathrm{d}s} = \kappa_\eta(\eta, \underline{\phi})[I_{\mathrm{b}\eta}(T) - I_\eta] - \sigma_{\mathrm{s}\eta}\left[I_\eta - \frac{1}{4\pi}\int_{4\pi} I_\eta(\hat{s}')\Phi_\eta(\hat{s},\hat{s}')\,\mathrm{d}\Omega'\right], \tag{2}$$

where it is assumed that Planck function $I_{\mathrm{b}\eta}$, scattering coefficient $\sigma_{\mathrm{s}\eta}$, and scattering phase function Φ_η are essentially constant across a small wavenumber interval $\Delta\eta$. We will reorder the absorption coefficient in Eq. (2) by multiplying the equation with Dirac's delta function $\delta(k - \kappa_\eta(\eta, \underline{\phi}_0))$, followed by integration over, and division by, $\Delta\eta$. Here $\kappa_\eta(\eta, \underline{\phi}_0)$ is the absorption coefficient evaluated at some (as of yet arbitrary) reference state $\underline{\phi}_0 = (T = T_0,\ p = p_0,\ \underline{x} = \underline{x}_0)$. This leads to

$$\frac{\mathrm{d}I_k}{\mathrm{d}s} = k^*(\underline{\phi}, k)[f(\underline{\phi}_0, k)I_{\mathrm{b}\eta} - I_k)] - \sigma_{\mathrm{s}\eta}\left(I_k - \frac{1}{4\pi}\int_{4\pi} I_k(\hat{s}')\Phi_\eta(\hat{s},\hat{s}')\,\mathrm{d}\Omega'\right) \tag{3}$$

provided that at every wavenumber where $\kappa_\eta(\eta, \underline{\phi}_0)$ has one and the same value k, $\kappa_\eta(\eta, \underline{\phi})$ always also has one unique value $k^*(\underline{\phi}, k)$. If the absorption coefficient behaves in such a way, then the intensity I_η will also always be the same for all these wavenumbers, and

$$I_k = \frac{1}{\Delta\eta}\int_{\Delta\eta} I_\eta(\eta)\delta(k - \kappa_\eta(\eta, \underline{\phi}_0))\,\mathrm{d}\eta = I_k(k) f(\underline{\phi}_0, k), \tag{4}$$

where $f(\underline{\phi}_0, k)$ is the k-distribution, and is evaluated as

$$\begin{aligned} f(\underline{\phi}_0, k) &= \frac{1}{\Delta\eta}\int_{\Delta\eta} \delta(k - \kappa_\eta(\eta, \underline{\phi}_0))\,\mathrm{d}\eta = \frac{1}{\Delta\eta}\sum_i \int \delta(k - \kappa_\eta(\eta, \underline{\phi}_0))\,\frac{\mathrm{d}\eta}{\mathrm{d}\kappa_\eta}\,\mathrm{d}\kappa_\eta \\ &= \frac{1}{\Delta\eta}\sum_i \left|\frac{\mathrm{d}\eta}{\mathrm{d}\kappa_\eta}\right|(\eta_i, \underline{\phi}_0). \end{aligned} \tag{5}$$

In this relation, the summation is over all occurrences where $\kappa_\eta(\eta, \underline{\phi}_0) = k$, as illustrated in Fig. 1 (the absolute value signs stem from the fact that, if $\mathrm{d}\eta/\mathrm{d}\kappa_\eta < 0$, then also $\mathrm{d}\kappa_\eta < 0$). Similarly, one can obtain the k-distribution for the local state $\underline{\phi}$, or

$$f(\underline{\phi}, k^*) = \frac{1}{\Delta\eta}\sum_i \left|\frac{\mathrm{d}\eta}{\mathrm{d}\kappa_\eta}\right|(\eta_i, \underline{\phi}), \tag{6}$$

which has identical k^*–κ_η intersection wavenumbers η_i, as also indicated in Fig. 1. Eq. (6) may also be rewritten as

$$f(\underline{\phi}, k^*) = \frac{1}{\Delta\eta}\sum_i \left|\frac{\mathrm{d}\eta}{\mathrm{d}\kappa_\eta}\right|(\eta_i, \underline{\phi}_0)\left|\frac{\mathrm{d}\kappa_\eta(\underline{\phi}_0)}{\mathrm{d}\kappa_\eta(\underline{\phi})}\right|. \tag{7}$$

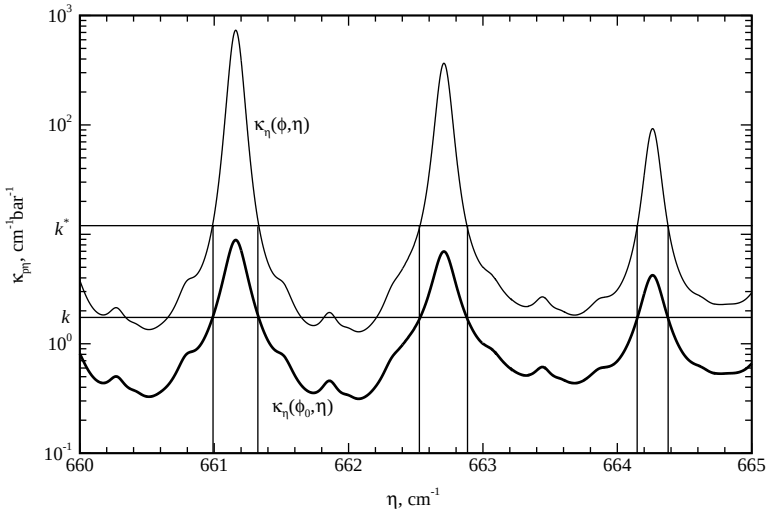

Fig. 1. Extraction of k-distributions from spectral absorption coefficient data (thick line is for CO_2 in nitrogen, across a small portion of the CO_2 15 μm band, $p = 1.0$ bar, $T = 296$ K; thin line is artificial).

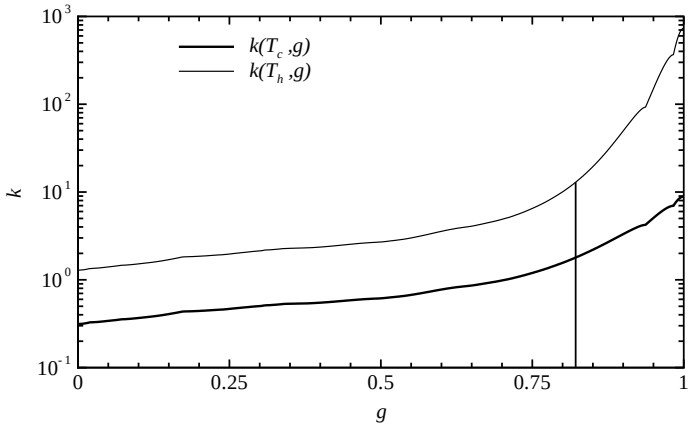

Fig. 2. Reordered absorption coefficients from Fig. 1 vs. cumulative k-distribution g.

Since $\kappa_\eta(\underline{\phi})(=k^*)$ is a unique function of $\kappa_\eta(\underline{\phi}_0)(=k)$, we have

$$f(\underline{\phi}, k^*)\,\mathrm{d}k^* = f(\underline{\phi}_0, k)\,\mathrm{d}k \tag{8}$$

provided that $\mathrm{d}k^*/\mathrm{d}k \geqslant 0$ everywhere, i.e., $\kappa_\eta(\underline{\phi})$ must be a uniformly increasing function of $k = \kappa_\eta(\underline{\phi}_0)$. The cumulative k-distribution g is then identical for both cases, i.e.,

$$g(\underline{\phi}_0, k) = \int_0^k f(\underline{\phi}_0, k)\,\mathrm{d}k = \int_0^{k^*} f(\underline{\phi}, k^*)\,\mathrm{d}k^* = g(\underline{\phi}, k^*). \tag{9}$$

Eq. (9) may be inverted for both k and k^*, with both being a function of the same cumulative k-distribution g, as indicated in Fig. 2. This is the definition of *correlated k-distributions*. Intensity

averaged over the interval $\Delta\eta$ then follows as

$$\frac{1}{\Delta\eta}\int_{\Delta\eta} I_\eta \,\mathrm{d}\eta = \int_0^\infty I_k \,\mathrm{d}k = \int_0^1 I_g \,\mathrm{d}g, \tag{10}$$

where I_g is the solution to the standard RTE

$$\frac{\mathrm{d}I_g}{\mathrm{d}s} = k^*(\underline{\phi}, g)(I_{\mathrm{b}\eta} - I_g) - \sigma_{\mathrm{s}\eta}\left(I_g - \frac{1}{4\pi}\int_{4\pi} I_g(\hat{s}')\Phi_\eta(\hat{s},\hat{s}')\,\mathrm{d}\Omega'\right). \tag{11}$$

A special case of the correlated-k distribution occurs when the absorption coefficient is *scaled*: this implies that, from Eq. (1), the ratio k^*/k is independent of k, and Eq. (11) reduces to

$$\frac{\mathrm{d}I_g}{\mathrm{d}s} = k(\underline{\phi}_0, g)u(\underline{\phi}, \underline{\phi}_0)(I_{\mathrm{b}\eta} - I_g) - \sigma_{\mathrm{s}\eta}\left(I_g - \frac{1}{4\pi}\int_{4\pi} I_g(\hat{s}')\Phi_\eta(\hat{s},\hat{s}')\,\mathrm{d}\Omega'\right). \tag{12}$$

At first glance, Eq. (11) looks superior to Eq. (12), since the assumption of a scaled absorption coefficient is more restrictive. However, in practice one needs to approximate an actual absorption coefficient, which is neither scaled nor correlated: if the scaling method is employed, the scaling function $u(\underline{\phi}, \underline{\phi}_0)$ can be freely chosen and, thus, optimized for a problem at hand. On the other hand, if the correlated-k method is used, the absorption coefficient is simply *assumed* to be correlated (even though it is not), and the inherent error cannot be minimized.

2.2. Full spectrum analysis

Following the treatment of Modest and Zhang [10] for a scaled absorption coefficient, the analysis is quite similar for full-spectrum, correlated k-distributions. As for any global method, we must now assume that scattering properties (and wall reflectances) are gray. We then reorder Eq. (2) by first multiplying with $\delta(k - \kappa_\eta(\eta, \underline{\phi}_0))$, followed by integration over the *entire* spectrum. This leads to

$$\frac{\mathrm{d}I_k}{\mathrm{d}s} = k^*(\underline{\phi}, k)[f(T, \underline{\phi}_0, k)I_{\mathrm{b}}(T) - I_k] - \sigma_{\mathrm{s}}\left(I_k - \frac{1}{4\pi}\int_{4\pi} I_k(\hat{s}')\Phi(\hat{s},\hat{s}')\,\mathrm{d}\Omega'\right) \tag{13}$$

again provided that at every wavenumber across the entire spectrum, where $\kappa_\eta(\eta, \underline{\phi}_0) = k$, we must also have a unique value for $\kappa_\eta(\eta, \underline{\phi}) = k^*(\underline{\phi}, k)$ (which may be a function of k, but not of η). In Eq. (13) I_k and f are defined as

$$I_k = \int_0^\infty I_\eta \delta(k - \kappa_\eta(\eta, \underline{\phi}_0))\,\mathrm{d}\eta, \tag{14}$$

$$f(T, \underline{\phi}_0, k) = \frac{1}{I_{\mathrm{b}}}\int_0^\infty I_{\mathrm{b}\eta}(T)\delta(k - \kappa_\eta(\eta, \underline{\phi}_0))\,\mathrm{d}\eta. \tag{15}$$

Therefore, in this context f is a Planck function weighted, full-spectrum k-distribution, which—besides the reference conditions $\underline{\phi}_0$—depends on temperature through the Planck function. Similar to the narrow band case we find

$$f(T, \underline{\phi}_0, k) = \frac{1}{I_{\mathrm{b}}(T)}\sum_i I_{\mathrm{b}\eta i}(T)\left|\frac{\mathrm{d}\eta}{\mathrm{d}\kappa_\eta}\right|(\eta_i, \underline{\phi}_0) \tag{16}$$

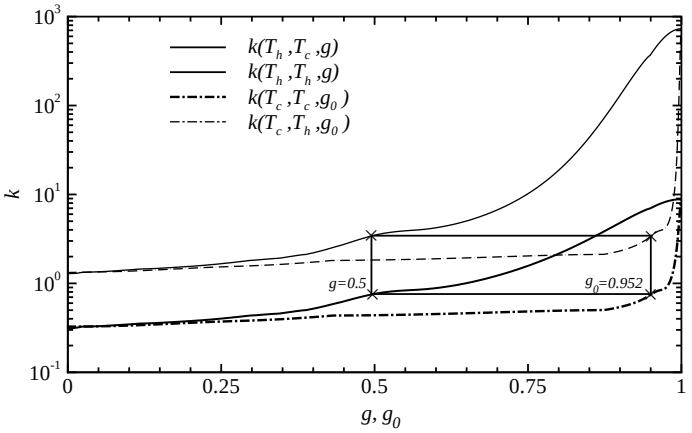

Fig. 3. k-distribution equivalence of correlated absorption coefficients for varying Planck function temperatures.

and again, if $\kappa_\eta(\eta, \underline{\phi})$ is a monotonically increasing function of $k = \kappa_\eta(\eta, \underline{\phi}_0)$, then

$$f(T, \underline{\phi}_0, k)\,\mathrm{d}k = f(T, \underline{\phi}, k^*)\,\mathrm{d}k^* \tag{17}$$

and the k-distributions are correlated, i.e.,

$$g(T, \underline{\phi}_0, k) = \int_0^k f(T, \underline{\phi}_0, k)\,\mathrm{d}k = \int_0^{k^*} f(T, \underline{\phi}, k^*)\,\mathrm{d}k^* = g(T, \underline{\phi}, k^*). \tag{18}$$

Total intensities I can then be obtained by integrating the I_k found from Eq. (13) over k-space. This is inconvenient, in particular since $f(T, \underline{\phi}_0, k)$ is a very ill-behaved function [10], just like narrow band k-distributions. On the other hand, because of its dependence on local temperature, f cannot be divided out as was done in the narrow band case, in order to integrate over the more convenient g-space. This can be overcome by dividing Eq. (13) by the k-distribution evaluated at the reference temperature, $f(T_0, \underline{\phi}_0, k)$, leading to

$$\frac{\mathrm{d}I_g}{\mathrm{d}s} = k^*(T_0, \underline{\phi}, g_0)[a(T, T_0, g_0)I_\mathrm{b}(T) - I_g] - \sigma_\mathrm{s}\left(I_g - \frac{1}{4\pi}\int_{4\pi} I_g(\hat{s}')\Phi(\hat{s}, \hat{s}')\,\mathrm{d}\Omega'\right) \tag{19}$$

together with

$$I_g = I_k / f(T_0, \underline{\phi}_0, k) = \int_0^\infty I_\eta \delta(k - \kappa_\eta(\eta, \underline{\phi}_0))\,\mathrm{d}\eta / f(T_0, \underline{\phi}_0, k), \tag{20}$$

$$g_0(T_0, \underline{\phi}_0, k) = \int_0^k f(T_0, \underline{\phi}_0, k)\,\mathrm{d}k, \tag{21}$$

$$a(T, T_0, g_0) = \frac{f(T, \underline{\phi}_0, k)}{f(T_0, \underline{\phi}_0, k)} = \frac{\mathrm{d}g(T, \underline{\phi}_0, k)}{\mathrm{d}g_0(T_0, \underline{\phi}_0, k)}. \tag{22}$$

In Eq. (22) numerator and denominator are both evaluated at identical values of k (as indicated in Fig. 3), which in turn is related to g_0 through Eq. (21). Note also that the weight function $a(T, T_0, g_0)$ is independent of $\underline{\phi}_0$ (for a truly correlated absorption coefficient) from Eq. (17).

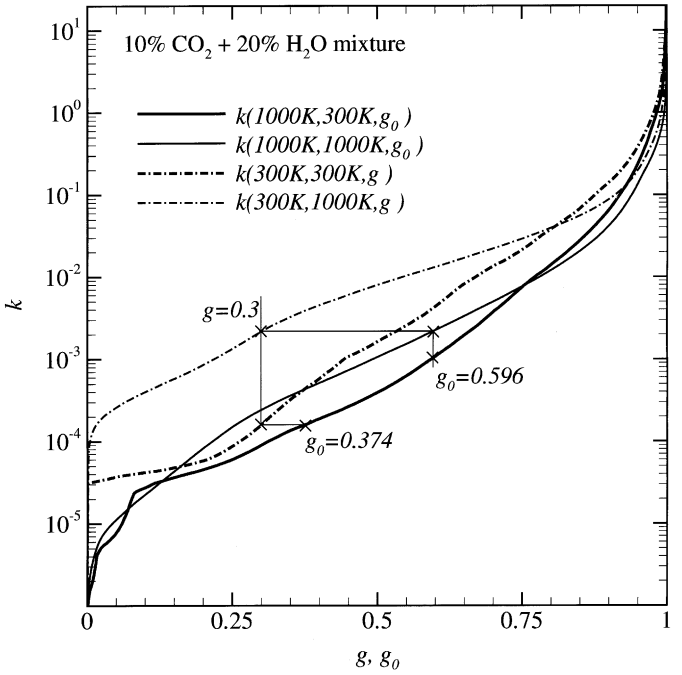

Fig. 4. (Lack of) k-distribution equivalence for varying Planck function temperatures for real gas mixtures (CO_2–H_2O–nitrogen mixture at different temperatures using HITEMP: $T_h = 1000$ K, $T_c = 300$ K, uniform $p = 1$ bar, $x_{CO_2} = 0.1$, $x_{H_2O} = 0.2$).

While k^* is, for a truly correlated absorption coefficient, a function of composition variables $\underline{\phi}$ and k only, such a relation is not known; instead we *assume* an actual absorption coefficient to *be* correlated. I.e., we assume Eq. (18) to hold for the actual absorption coefficient, or

$$k^*(\underline{\phi}, k) = k^*(T, \underline{\phi}, g), \tag{23}$$

where g is the cumulative k-distribution for the absorption coefficient at reference state $\underline{\phi}_0$ [left half of Eq. (18)]. However, the reordered spectral variable for Eq. (19) is g_0, i.e., the cumulative k-distribution for, both, absorption coefficient and Planck function evaluated at the reference state. Since $k(T, \underline{\phi}_0, g)$ and $k(T_0, \underline{\phi}_0, g_0)$ are both reordering the same absorption coefficient (but using different weight functions), $k(T_0, \underline{\phi}_0, g_0)$ is simply stretched in g-space, as shown in Fig. 3 (The four k-distributions in Fig. 3 where obtained from the two absorption coefficient distributions of Fig. 3, after spreading their spectral range across the entire spectrum, for Planck function temperatures of 300 and 1000 K). Since Eq. (18) can be applied at any temperature, including $T = T_0$, it is clear that $k^*(T_0, \underline{\phi}, g_0)$ is stretched in exactly the same way, or

$$k^*(\underline{\phi}, k) = k^*(T, \underline{\phi}, g) = k^*(T_0, \underline{\phi}, g_0). \tag{24}$$

Note that Eq. (24) is exact only for a truly correlated absorption coefficient: Fig. 4 shows the equivalent four k-distributions for a 10% CO_2–20% H_2O–70% nitrogen mixture evaluated from the HITEMP database [6]: if the k-distributions $k(T = 300\text{ K}, T_0 = 1000\text{ K}, g)$ (Planck function evaluated at 300 K, absorption coefficient at 1000 K) and $k(T = 300\text{ K}, T_0 = 300\text{ K}, g)$ (Planck function at

300 K, κ_η at 300 K) were correlated, then, from Eq. (18), they should also be correlated for a Planck function evaluated at 1000 K. This implies that for any value of g (here shown for $g = 0.3$) the two k-values at one Planck function temperature (here 300 K) should map to identical g_0-values at any other Planck function temperature (here $T_0 = 1000$ K). This is clearly not the case for the given carbon dioxide–water vapor mixture. However, a graph such as Fig. 4 can be employed to investigate how close to correlatedness an absorption coefficient actually is.

Returning to Eq. (19), the total intensity is evaluated from

$$I = \int_0^\infty I_\eta \, \mathrm{d}\eta = \int_0^\infty I_k \, \mathrm{d}k = \int_0^1 I_g \, \mathrm{d}g_0. \tag{25}$$

As for the narrow band k-distributions the problem is reduced to a single k-distribution if a scaled absorption coefficient is employed. Then the k^*-term in Eq. (19) is replaced by

$$k^*(T, \underline{\phi}, g) = k(T, \underline{\phi}_0, g) u(\underline{\phi}, \underline{\phi}_0) = k(T_0, \underline{\phi}_0, g_0) u(\underline{\phi}, \underline{\phi}_0). \tag{26}$$

3. Reference state and scaling function

Whether the assumption of a correlated absorption coefficient is to be used, or whether the absorption coefficient is to be scaled, the exact k vs. g behavior can be employed for only a single reference state $\underline{\phi}_0$. Therefore, the choice of $\underline{\phi}_0$ is very important and should be optimized for any given problem. Modest and Zhang [10] suggest, for a medium at constant pressure p,

$$\underline{x}_0 = \frac{1}{V} \int_V \underline{x} \, \mathrm{d}V, \tag{27}$$

$$\kappa_\mathrm{P}(T_0, \underline{x}_0) = \frac{1}{V} \int_V \kappa_\mathrm{P}(T, \underline{x}) I_\mathrm{b}(T) \, \mathrm{d}V, \tag{28}$$

i.e., volume-averaged mole fraction and a Planck-mean temperature based on average emission from the volume. Similar arguments can also be used for narrow band distributions, for which Eq. (28) is then replaced by

$$\overline{\kappa_\eta}(T_0, \underline{x}_0) I_{\mathrm{b}\eta}(T_0) = \frac{1}{V} \int_V \overline{\kappa_\eta}(T, \underline{x}) I_{\mathrm{b}\eta}(T) \, \mathrm{d}V, \tag{29}$$

where $\overline{\kappa_\eta} = \int_{\Delta\eta} \kappa_\eta \, \mathrm{d}\eta / \Delta\eta$ is the average absorption coefficient.

In the correlated-k method, the $k(T, \underline{\phi}_0, g)$ are then determined, followed by evaluation of $k^* = k(T, \underline{\phi}, g)$ making the assumption of corresponding g-values (and its resulting errors). If a scaled absorption coefficient is to be used, scaling functions must be found, and Modest and Zhang [10] suggest the implicit relation

$$\int_0^\infty I_{\mathrm{b}\eta}(T_0) \exp(-\kappa_\eta(\eta, \underline{\phi}) L_\mathrm{m}) \, \mathrm{d}\eta = \int_0^\infty I_{\mathrm{b}\eta}(T_0) \exp[-\kappa_\eta(\eta, \underline{\phi}_0) u(\underline{\phi}, \underline{\phi}_0) L_\mathrm{m}] \, \mathrm{d}\eta, \tag{30}$$

i.e., equating radiation leaving from a homogeneous slab of mean beam length, L_m. Using k-distributions this becomes

$$\int_0^1 \exp[-k^*(T_0, \underline{\phi}, g) L_\mathrm{m}] \, \mathrm{d}g = \int_0^1 \exp[-k(T_0, \underline{\phi}_0, g_0) u(\underline{\phi}, \underline{\phi}_0) L_\mathrm{m}] \, \mathrm{d}g_0. \tag{31}$$

Eq. (31) is readily inverted through a Newton–Raphson scheme: first the left-hand-side integral is evaluated (requiring about 10 quadrature points), and similarly the right-hand-side integral, starting with a guess of $u=1$; u and the right-hand-side integral are then updated until convergence (requiring some 3–5 iterations).

Both methods are about equally efficient numerically: besides the evaluation of $k(T,\underline{\phi}_0,g)$ [needed for both methods to evaluate $k(g_0)$ and the weight function a], for a correlated absorption coefficient k-distributions must be evaluated for all states $\underline{\phi}$ (with a Planck function based on the reference temperature). For a scaled absorption coefficient, the same k-distributions are needed, but here for the evaluation of the scaling functions u. The computational effort of inverting Eq. (31) is essentially negligible compared to the effort required for the evaluation of the k-distributions.

4. Sample calculations

To illustrate the validity of, both, correlated-k and scaled-k distributions, as well as their differences, a few simple (yet severe) examples will be considered, for narrow band as well as for full spectrum calculations. In all cases we will consider a slab of a hot gas (usually at 1000 K, unless stated otherwise), adjacent to a slab of cold gas (at 300 K). Both layers are at the same total and partial pressures.

For the narrow band calculations we will assume both layers to have equal thickness, and both a slab transmissivity and emissivity will be evaluated. The transmissivity for a blackbody beam $I_{b\eta}(T_h = 1000\,\mathrm{K})$, through such a double layer is [17]

$$\bar{\tau}_\eta = \frac{I_\eta(L)_{tr}}{I_{b\eta}(T_h)} = \frac{1}{\Delta\eta}\int_{\Delta\eta} \exp[-\kappa_\eta(T_h,x)L_h - \kappa_\eta(T_c,x)L_c]\,d\eta, \tag{32}$$

while the emissivity is defined here as the intensity of emitted radiation exiting the cold layer, as compared to the Planck function of the hot layer, or

$$\bar{\varepsilon}_\eta = \frac{I_\eta(L)_{em}}{I_{b\eta}(T_h)} = \frac{1}{\Delta\eta}\int_{\Delta\eta}\left[e^{-\kappa_\eta(T_c,x)L_c} - e^{-\kappa_\eta(T_c,x)L_c-\kappa_\eta(T_h,x)L_h} + \frac{I_{b\eta}(T_c)}{I_{b\eta}(T_h)}(1-e^{-\kappa_\eta(T_c,x)L_c})\right] d\eta. \tag{33}$$

Note that, while transmissivities are more regularly shown in the narrow band literature, the emissivity is generally more descriptive of heat transfer problems. Fig. 5 shows these narrow band transmissivities and emissivities for the 2.7 μm band of CO_2, as calculated by the LBL, scaled-k and correlated-k methods, using the HITEMP database [6], and all for a resolution of $\Delta\eta = 5\ \mathrm{cm}^{-1}$ (lines) and 25 cm^{-1} (symbols). The thickness of the layer is $L_h = L_c = 50$ cm, total pressure is 1 bar, and mole fraction is $x_{CO_2} = 0.1$. Both correlated and scaled k-distributions predict transmissivity very accurately with the exception of small discrepancies near the minima at 3600 and 3700 cm^{-1}. In absolute terms the error never exceeds 0.04 but, in relative terms, the error goes as high as 15%, since the error is largest near the band center, where transmissivities are small. Similar errors also show up in the emissivity, but the relative errors are somewhat amplified (with a maximum error of about 45%), since the emissivities are even smaller near the band centers. For both, transmissivity and emissivity, results from the two k-distributions are virtually identical, although correlated-k performs slightly better for the 2.7 μm band (in the case of the 4.3 μm band, not shown, roles are reversed

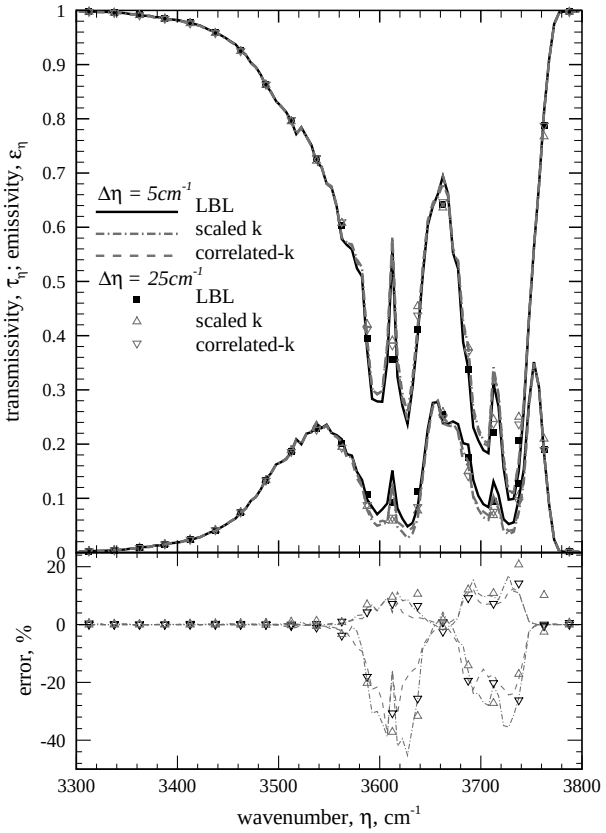

Fig. 5. Narrow band transmissivities and emissivities for the 2.7 μm band of CO_2, as calculated by the LBL, scaled K and correlated K methods.

and scaled-k slightly outperforms correlated-k). Fig. 6 shows transmissivities and emissivities for the wide 6.3 μm water vapor band. Conditions are the same as for Fig. 5, except that $x_{H_2O}=0.2$ and only a $\Delta\eta=25\ \mathrm{cm}^{-1}$ resolution is shown (a resolution of $5\ \mathrm{cm}^{-1}$ results in a very irregular shape which, while the k-distributions follow this behavior accurately, makes them difficult to compare). Again, both k-distributions predict transmissivities rather accurately, and the relative errors are somewhat amplified in the emissivities. And, again, both k-distributions give virtually the same results, both about equally accurate for this band. In summary, one may say that both models perform about equally well; this implies that—for narrow bands and for temperatures not exceeding 1000 K—the absorption coefficients for water vapor and carbon dioxide are relatively well correlated. Note also that the present case, with a sharp step in temperature, is rather extreme; accuracy can be expected to be significantly better in more realistic combustion systems.

To illustrate and compare the two k-distribution versions on a global or full-spectrum scale we will look at a mixture of $x_{CO_2}=0.1$ CO_2 and $x_{H_2O}=0.2$ H_2O, with a total pressure of 1 bar. As in the narrow band examples, we consider a hot layer ($T_h=1000$ and 2000 K, respectively; fixed thickness $L_h=50$ cm) adjacent to a cold layer ($T_c=300$ K; varying thickness L_c). Both sides of the slab are bounded by cold black walls. The heat flux leaving from the cold end of the slab is

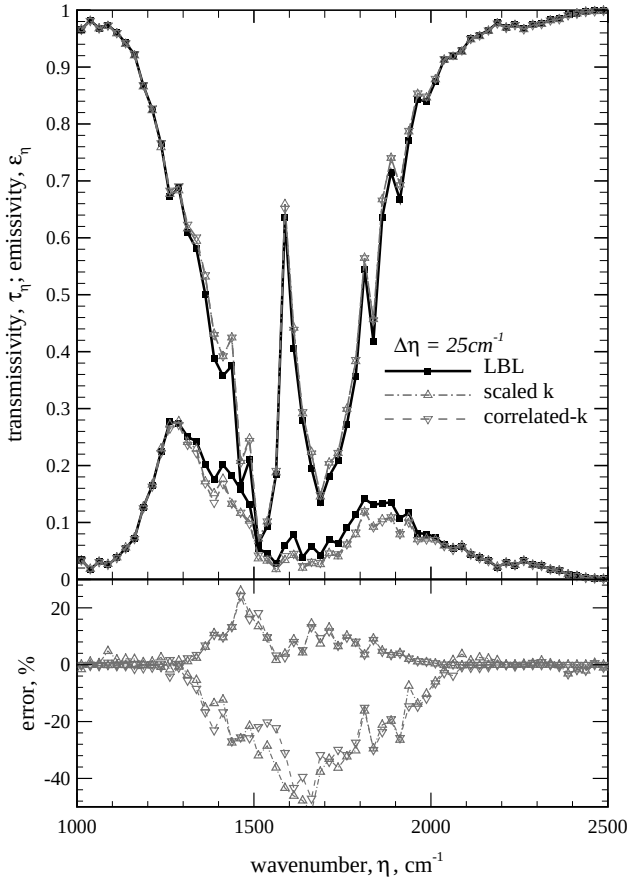

Fig. 6. Narrow band transmissivities and emissivities for the 6.3 μm band of water vapor, as calculated by the LBL, scaled K and correlated K methods.

then [17]

$$\frac{q}{\sigma T_{\mathrm{h}}^4} = \frac{1}{I_{\mathrm{bh}}} \int_0^\infty \{2[E_3(\kappa_\eta(T_{\mathrm{c}})L_{\mathrm{c}}) - E_3(\kappa_\eta(T_{\mathrm{c}})L_{\mathrm{c}} + \kappa_\eta(T_{\mathrm{h}})L_{\mathrm{h}})]I_{\mathrm{b}\eta}(T_{\mathrm{h}}) + [1 - 2E_3(\kappa_\eta(T_{\mathrm{c}})L_{\mathrm{c}})]I_{\mathrm{b}\eta}(T_{\mathrm{c}})\}\,\mathrm{d}\eta. \tag{34}$$

In terms of k-distributions, this becomes from Eqs. (19) and (26)

$$\frac{q}{\sigma T_{\mathrm{h}}^4} = \int_0^1 \left\{ 2[E_3(\tau_{g\mathrm{c}}) - E_3(\tau_{g\mathrm{c}} + \tau_{g\mathrm{h}})]a_g(T_{\mathrm{h}}) + [1 - 2E_3(\tau_{g\mathrm{c}})] \left(\frac{T_{\mathrm{c}}}{T_{\mathrm{h}}}\right)^4 a_g(T_{\mathrm{c}}) \right\} \mathrm{d}g, \tag{35}$$

where

$$\tau_{gi}(T_i) = \begin{cases} k^*(T_0, T_i, g_0)L_i & \text{for correlated-}k, \\ k(T_0, T_0, g_0)u(T_i, T_0)L_i & \text{for scaled-}k, \end{cases}$$

where $i = c$ or h, and with a_g from Eq. (22), T_0 from Eq. (28), and $u(T, T_0)$ from Eq. (31).

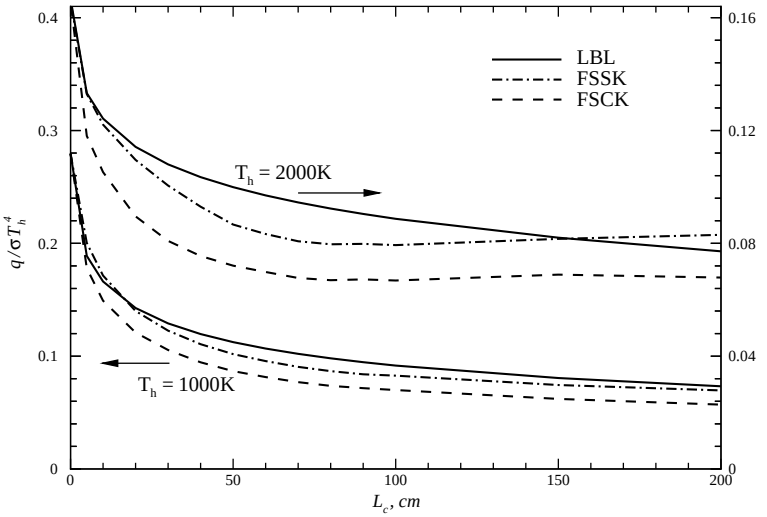

Fig. 7. Radiative flux exiting from the cold column of a two-column CO_2–H_2O–nitrogen mixture at different temperatures using HITEMP ($T_h = 1000$ and 2000 K, $L_h = 50$ cm; $T_c = 300$ K, L_c variable; uniform $p = 1$ bar, $x_{CO_2} = 0.1$, $x_{H_2O} = 0.2$, cold and black walls).

The results are shown in Fig. 7 for varying cold layer thickness. When there is no cold layer ($L_c = 0$), we only have a homogeneous hot layer, and both k-distribution versions reduce to the exact LBL results. For $L_c > 0$ correlated-k will always overpredict absorption in the cold layer and, thus, underpredict exiting heat flux. This is due to the fact that, for a correlated absorption coefficient, spectral regions with strong hot layer emission (large κ_η) are assumed to have also large absorption; this, however, is violated by the many "hot lines" at 1000 K and (much more so) at 2000 K. The scaled-k approximation, on the other hand, can optimize the (still correlated) k-distribution with the scaling function u, resulting in considerably smaller errors. Comparing with the narrow band results one may conclude that, while k-distributions are relatively correlated over small parts of the spectrum, this assumption becomes more tenuous when the entire spectrum is considered. Again, one should keep in mind that Fig. 7 depicts rather extreme examples. Modest and Zhang [10] have shown that, in two-dimensional combustion systems, the anticipated maximum error for FSSK is mostly below 3%.

5. Summary

In this paper a precise mathematical development of the correlated-k method has been given for narrow bands as well as for a global model. Differences and similarities between correlated and scaled absorption coefficients and their resulting k-distributions have been high-lighted and discussed. It was found that both methods require roughly the same numerical effort, although the correlated-k approach is perhaps a little more straightforward to implement. Narrow band results for CO_2 and H_2O, based on the HITEMP database, indicate that the absorption coefficient is relatively well correlated across small spectral regions, resulting in roughly equal accuracies for correlated and scaled k-distributions. It was observed that, for media with severe temperature nonuniformity, both methods predict transmissivity

of a gas column with great accuracy. Emissivities for such layers (of importance in combustion applications), exhibit slightly larger errors of up to 0.04 (which may result in locally relatively large errors on a percentage basis). For global models the absorption coefficient becomes less correlated, and the scaled k-distribution method (FSSK) distinctly outperforms its correlated cousin (FSCK). The reason for this is that, in the correlated-k method, the actual absorption coefficient, with its "hot lines" as given by HITEMP, is *assumed* to be correlated (although it is not). In the scaled-k method the scaling function is optimized, to mimic actual absorption coefficient behavior as closely as possible, resulting in more accurate results.

Acknowledgements

The author gratefully acknowledges the financial support of the National Science Foundation under contract CTS-9615009.

References

[1] Lacis AA, Oinas V. A description of the correlated-k distribution method for modeling nongray gaseous absorption, thermal emission, and multiple scattering in vertically inhomogeneous atmospheres. J Geophys Res 1991;96(D5):9027–63.
[2] Goody RM, Yung YL. Atmospheric radiation theoretical basis, 2nd ed. New York: Oxford University Press, 1989.
[3] Goody R, West R, Chen L, Crisp D. The correlated k method for radiation calculations in nonhomogeneous atmospheres. JQSRT 1989;42:539–50.
[4] Fu Q, Liou KN. On the correlated k-distribution method for radiative transfer in non-homogeneous atmospheres. J Atmos Sci 1992;49(22):2139–56.
[5] Rothman LS, Rinsland CP, Goldman A, Massie ST, Edwards DP, Flaud J-M, Perrin A, Camy-Peyret C, Dana V, Mandin J-Y, Schroeder J, McCann A, Gamache RR, Wattson RB, Yoshino K, Chance KV, Jucks KW, Brown LR, Nemtchinov V, Varanasi P. The HITRAN molecular spectroscopic database and HAWKS (HITRAN atmospheric workstation): 1996 Edition JQSRT 1998;60:665–710.
[6] Rothman LS, Camy-Peyret C, Flaud J-M, Gamache R, Goldman A, Goorvitch D, Hawkins R, Schroeder J, Selby J, Wattson R. HITEMP, the high-temperature molecular spectroscopic database 2000, available through http://www.hitran.com.
[7] Rivière P, Soufiani A, Taine J. Correlated-k and fictitious gas methods for H_2O near 2.7 μm. JQSRT 1992;48:187–203.
[8] Rivière P, Scutaru D, Soufiani A, Taine J. A new $c-k$ data base suitable from 300 to 2500 K for spectrally correlated radiative transfer in CO_2–H_2O transparent gas mixtures. In: Proceedings of the Tenth International Heat Transfer Conference. London: Taylor & Francis, 1994. p. 129–34.
[9] Rivière P, Soufiani A, Taine J. Correlated-k and fictitious gas model for H_2O infrared radiation in the Voigt regime. JQSRT 1995;53:335–46.
[10] Modest MF, Zhang H. The full-spectrum correlated-k distribution for thermal radiation from molecular gas-particulate mixtures. ASME J Heat Transfer 2002;124(1):30–8.
[11] Denison MK, Webb BW. A spectral line based weighted-sum-of-gray-gases model for arbitrary RTE solvers. ASME J Heat Transfer 1993;115:1004–12.
[12] Denison MK, Webb BW. The spectral-line-based weighted-sum-of-gray-gases model in nonisothermal nonhomogeneous media. ASME J Heat Transfer 1995;117:359–65.
[13] Hottel HC, Sarofim AF. Radiative transfer. New York: McGraw-Hill, 1967.
[14] Modest MF. The weighted-sum-of-gray-gases model for arbitrary solution methods in radiative transfer. ASME J Heat Transfer 1991;113(3):650–6.

[15] Rivière P, Soufiani A, Perrin Y, Riad H, Riad AG. Air mixture radiative property modelling in the temperature range 10000–40000 K. JQSRT 1996;56:29–45.
[16] Pierrot L, Rivière P, Soufiani A, Taine J. A fictitious-gas-based absorption distribution function global model for radiative transfer in hot gases. JQSRT 1999;62:609–24.
[17] Modest MF. Radiative heat transfer. New York: McGraw-Hill, 1993.